Aquifers, Faults, Subsidence, and Lightning Databases

Kathleen S. Haggar, Les R. Denham, and H. Roice Nelson, Jr.

Dynamic Measurement LLC., 16515 Hedgecroft, Ste. 320, Houston, Texas 77060

ABSTRACT

In discussing characteristics of aquifers, faulting, subsidence, and lightning databases, we recognized similar measurement and monitoring issues and solutions.

Lightning data occurs everywhere, covering the spatial extent of aquifers. In this paper, we highlight lightning attribute maps at regional and prospect scales, and relate these maps to aquifer and subsidence maps. Lightning strikes cluster, these clusters are somewhat consistent over time, and the resulting lineaments tie to fault lines. Lightning strikes are impacted by earth tides, and the impact of tides on marshes and swamps increases with increasing subsidence.

Lightning databases open new ways to measure and monitor natural resources, including aquifers, faults, and subsidence. Lightning data are evergreen, in that new lightning strike measurements are added to lightning databases every time there is a thunderstorm. Lightning strikes are primarily controlled by earth currents. Earth currents are modified by aquifers (resistive, if fresh water, and more conductive with increased salinity), faults (disrupting lateral flow of electrons along conductive layers), and subsidence (changes in compaction change conductivity).

INTRODUCTION

Lightning occurs everywhere and public and private databases enable analysis of accumulation of lightning strike density and lightning strike attributes. This Texas analysis includes two areas, one covering Colorado County, Texas, between 96 degrees 53 minutes and 96 degrees 6 minutes west longitude, and between 29 degrees 12 minutes and 30 degrees north latitude, and the second area covering parts Austin, Waller, Ft. Bend, and Harris counties, Texas (Fig. 1) between 96 degrees 15 minutes and 95 degrees west longitude, and between 29 degrees 36 minutes and 30 degrees 6 minutes north latitude.

Figure 1 also includes a merged map of temperature gradients over these two areas. Recently the Texas Bureau of Economic Geology provided public domain bottom hole temperature data for the areas being evaluated. Cross-plots of lightning strike density against temperature gradient show strong correlation, as will be described more completely later. Several lightning attributes show a similar correlation with temperature gradient.

For context, these lightning analysis areas are within the boundaries of major and minor aquifers, as shown in Figure 2 (Ewing, 1990; George et al., 2011). These aquifers include the Gulf Coast Aquifer, the Yegua-Jackson Aquifer, and the Brazos River Alluvium Aquifer. Aquifer distribution and sand percentages illustrate the heterogeneity of Gulf Coast deposition. These lateral changes in lithology are overlaid by other geologic processes like subsidence. Figure 3 is a map of the rate of subsidence in the Houston-Galveston area prepared by the Houston Galveston Subsidence District (2000). It is interesting to note the most rapid subsidence is on the downthrown side of listric faults, which Ewing (1990) shows are at the northwest of and therefore must die out under Galveston Bay. Haggar (2014, this volume) showed how a relative minor rise in sea level increases weight on Gulf Coast sediments, like are found under Galveston Bay, speeding up fluid expulsion, compaction, reactivation of faulting, and the rate of movement along growth faults, and thus increasing the rate of subsidence. Jin et al. (2013) demonstrated a relationship between lightning strikes and areas of active faulting.

Similar to how aquifer levels are measured and monitored, and how rates of subsidence are measured and monitored, lightning strike data is being continually collected and stored. The primary reasons for collecting and

Haggar, K, S., L. R. Denham, and H. R. Nelson, Jr, 2014, Aquifers, faults, subsidence, and lightning databases: Gulf Coast Association of Geological Societies Transactions, v. 64, p. 161–177.

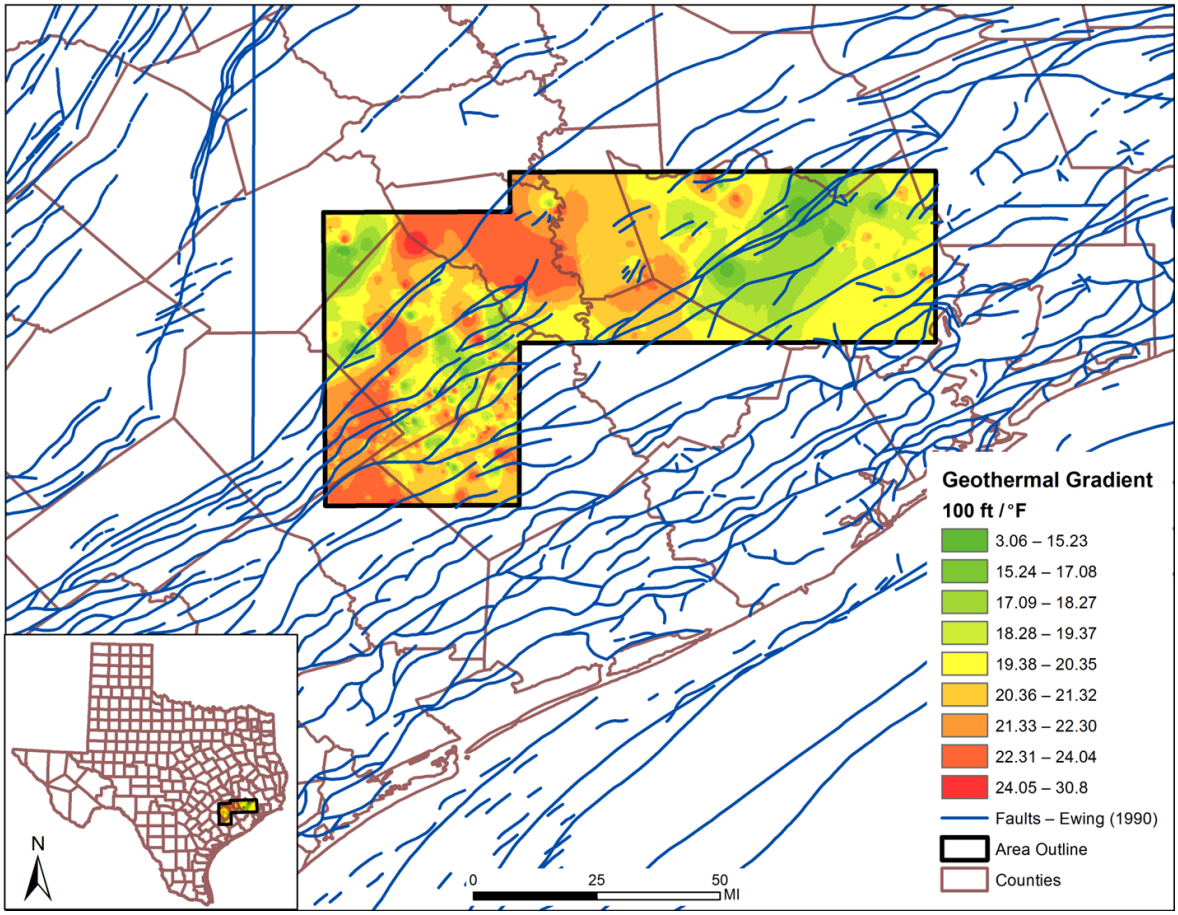

Figure 1. The geothermal gradient is colored within two rectangular analysis areas referenced in this paper, which areas cover (1) Colorado County, Texas, and (2) parts of Austin, Waller, Ft. Bend, and Harris counties in Texas.

storing lightning data has been for insurance, meteorological, and safety reasons. Only over the last 6 years has it been recognized how maps of lightning strike locations, density, and attributes are related to subsurface geology. This paper summarizes relationships discovered so far.

For instance, Dynamic Measurement LLC (DML) has learned to routinely calculate earth tides and to tie each lightning strike to the earth tide resulting from integrating lunar and solar gravity effects on the earth. From North Dakota to Texas there are from 20–50% more lightning strikes during periods of most rapid change of earth tide than there are when the tide is not changing. This is illustrated in Figure 4 (left) for a project in Texas. Our interpretation is tides open or close faults a little bit, and increase conductivity, or possibly increase seeps. Figure 4 (right) shows the results for a swampy area near the Gulf Coast. There is a similar increase in the number of strikes approaching the maximum rate of flood. However, in this area there are no lightning strikes over 15 years at either the maximum flood or maximum ebb of the combined earth and solar tides. The earth tides are known to move water up and down in water wells in this area, and the current interpretation is biogenic gases are being washed out by the tides, leaving no escaping methane to disrupt the atmospheric dielectric at maximum ebb and flood.

Lightning strike locations and attributes are primarily controlled by geology. This paper starts to explore the impact of the geologic characteristics of aquifers and proposes aquifer depletion impacts subsidence, changes the electrical characteristics of the earth, and impacts lightning strike locations and attributes. Even though DML has studied the relationship between lightning and geology for several years, there are many earth characteristics to consider and integrate into analysis of this new geophysical data type.

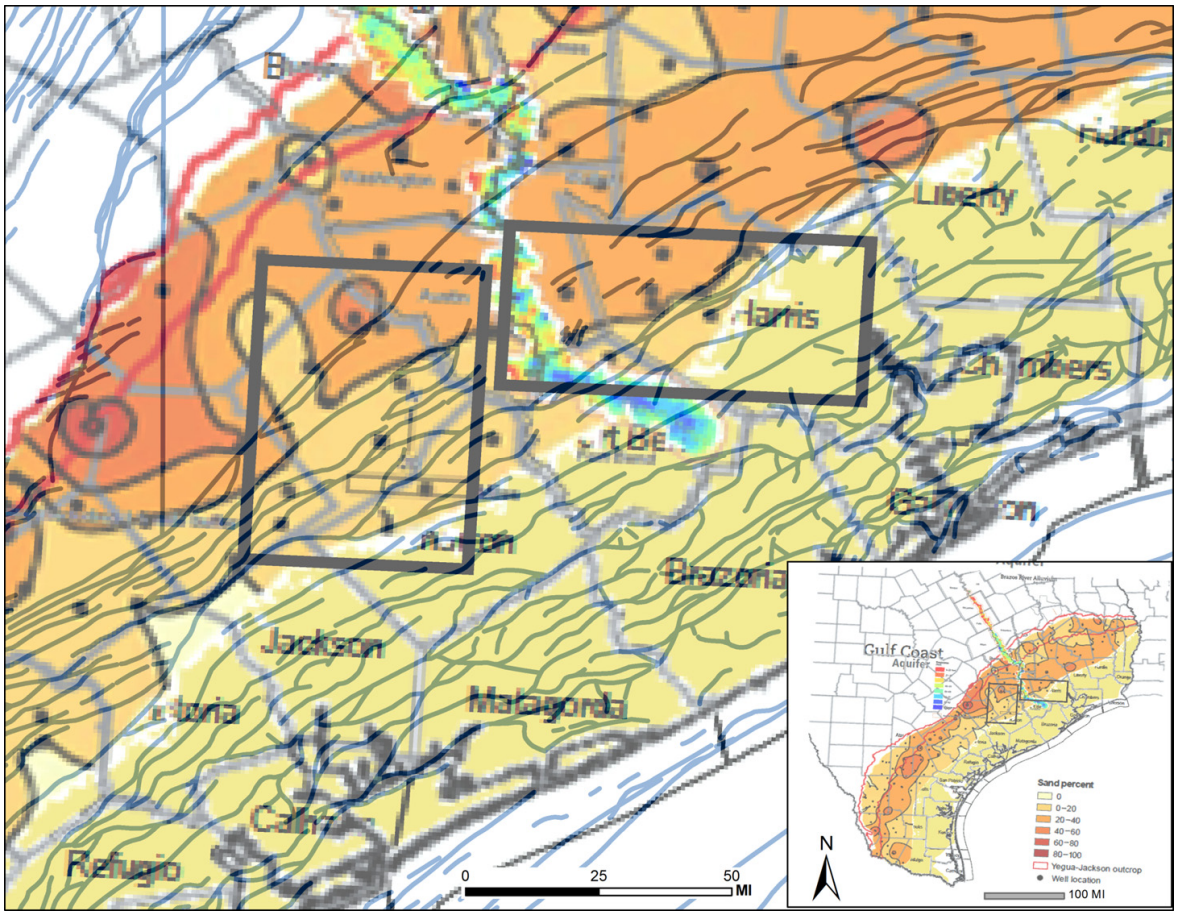

Figure 2. The area referenced is in the northern middle of the Gulf Coast Aquifer, merged here with the Carrizo, Trinity, and Edwards aquifers. The Brazos River Alluvium Aquifer thickness is shown along with the faults and salt domes (Ewing, 1990; George et al., 2011). Also, notice the straight path of the Brazos River aligned to the Brazos Transform.

HISTORY

The lightning strike records were collected at first for meteorological purposes: early storm warning, safety, and for weather reports. Dr. Richard E. Orville, now at Texas A&M University, started the NLDN (National Lightning Detection Network) in March 1982, when at the State University of New York in Albany. The NLDN has been in continuous operation by Vaisala, Inc. since January 1989 (Orville, 2008). The data collection and processing procedures are described in meteorological literature (Murphy et. al., 2008; Baba and Rakov, 2008).

Insurance companies found out this data was available, and used it to validate damage claims such as houses burning down, destroyed transformers, and electrical damage inside houses at the time of the lightning storms. Supporting insurance companies became an ongoing funding source for operations and development of the privately owned NLDN. In the early 1980s, up to 60% of insurance claims for homes damaged or destroyed by lightning were found to be fraudulent or misrepresented (Orville, 2012).

DML has been evaluating the implications of lightning strike locations, density, and lightning attribute maps on natural resource exploration since 2008. Vaisala, Inc. introduced the GLD–360 (Global Lightning Database)

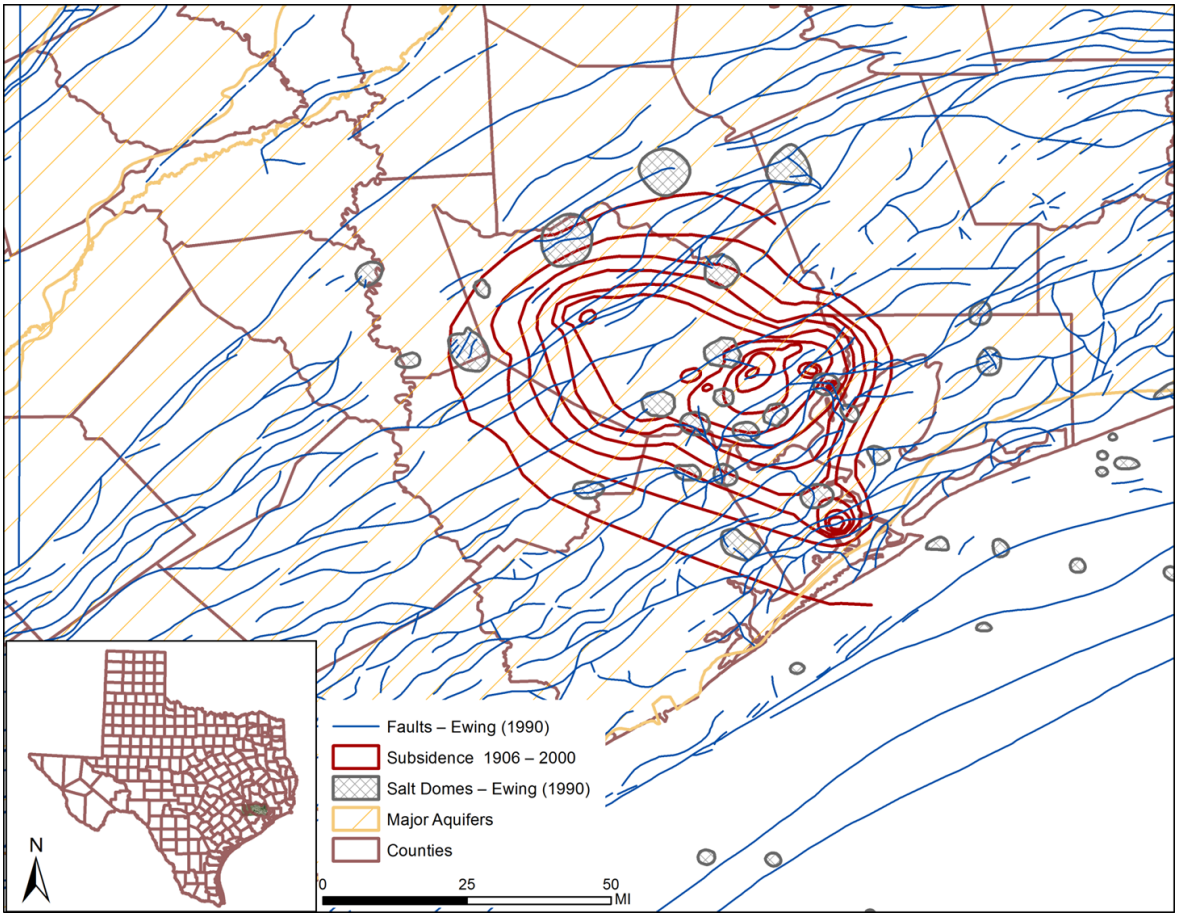

Figure 3. Subsidence in the Houston Galveston Subsidence District (HGSD) from 1906–2000 (Houston Galveston Subsidence District, 2000), with delineation of faults and salt domes (Ewing, 1990).

worldwide lightning database in 2011 (Hembury and Holle, 2011). There are 330 ground based sensors in the NLDN. The GLD–360 network consists of a combination of satellite and ground based sensors. Private networks, like the NLDN, can be set up in numerous parts of the world. The NLDN database includes the location of the lightning strike, with 60–100 meter resolution within the continental United States, while the GLD–360 database has kilometer resolution elsewhere in the world.

In Texas, each lightning strike is typically recorded by 8–14 sensors. These sensors record the time each strike occurs with microsecond (10^{-6} seconds) accuracy. Attributes measured by the various sensors are reconciled and a quality measurement recorded called chi squared is calculated. Attributes measured by the NLDN include polarity, rise time (the time to go from background electrical noise to the peak current), peak current, and peak-to-zero time (the time to back down to the background electrical noise). Figure 5 is a cartoon describing the lightning waveform. Most lightning strikes have negative polarity, as illustrated, and come from the bottom of thunderclouds. Positive polarity lightning strikes tend to come at the end of a thunderstorm and tend to have higher peak current, coming from the top of thunderclouds. From these attributes are calculated total wavelet time, wavelet symmetry, surface resistivity, resistivity volumes, and other lightning attributes. The key lightning attribute measured and recorded by the GLD–360 is peak current.

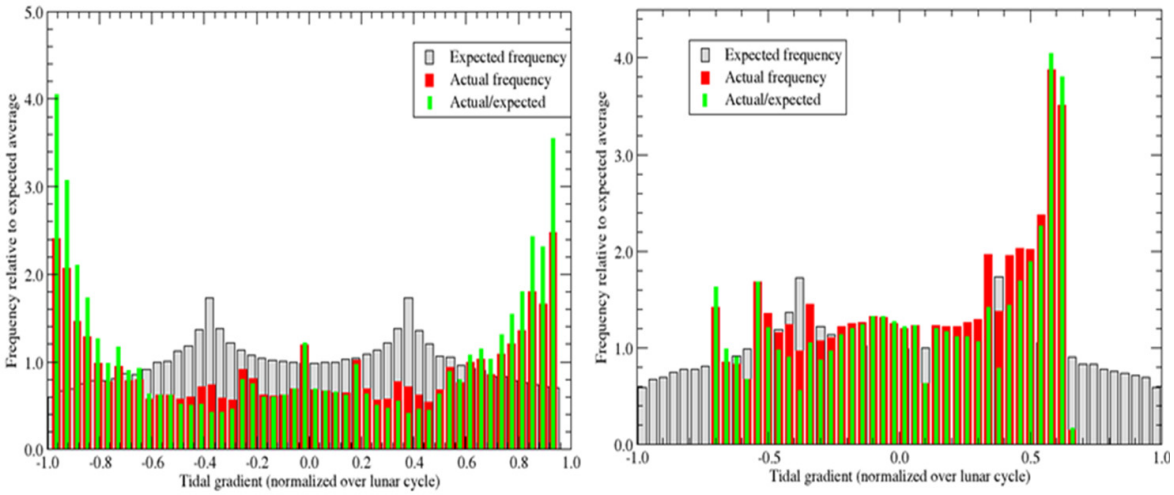

Figure 4. The left image is from Texas showing there are more lightning strikes at both the maximum ebb and maximum flow of earth tides. The right image is from Florida showing there are no lightning strikes over 15 years at maximum ebb or maximum flow of earth tides, although there are significantly more strikes just past half flood.

THEORY

Lightning is a meteorological phenomenon. The static electricity build-up associated with a lightning strike is tied to particle movement in thunderstorms. When this static charge becomes high enough it bridges the resistant atmospheric dielectric (Rakov and Uman, 2003). Lightning strokes can go 200 kilometers cloud-to-cloud, before becoming a cloud-to-ground strike (Hembury, 2011). These strikes normalize the earth's capacitor, which at the megascale consists of the ionosphere and the top of the mantle by the Mohorovicic discontinuity.

Geophysicists have known about telluric or earth currents since the early 1950s, when the magnetotelluric technique was introduced by the French geophysicist Louis Cagniard (1953) and Russian geophysicist Andrey Nikolayevich Tikhonov. It has also been known the earth currents are charged by lightning storms from other places around the world. What was not realize until the work being documented here was that cloud-to-ground strike locations are largely controlled by terra levis (shallow earth) currents that are fed by both lightning strikes and the deeper telluric currents (Nelson, Seibert, and Denham, 2014).

Figure 6 illustrates how lightning can be considered a RC (resistance-capacitor) circuit, where voltage (out) is the lightning stroke, and V (in) is the static voltage or charge accumulating in the thunderstorm. C is the capacitor formed by the atmospheric static charge (usually at or near the bottom of the cloud for negative strikes, and at or near the top of thunderclouds for positive strikes) as one plate, with the atmosphere as the dielectric, and the conducting ground as the other plate. R1 is the resistance of the earth below the thundercloud, as it affects the build-up of static charge within the thundercloud. R2 is the resistance of the earth below the cloud as it affects the movement of electrons to re-balance static charges after the lightning completes the circuit. Denham and Siebert (2014) have submitted an abstract to the 2014 SEG to review the mathematics of calculating surface resistivity and resistivity volumes from NLDN lightning strike data.

EXAMPLES

DML has completed more than a dozen different lightning analysis projects, from North Dakota to Michigan to New York to Florida to Texas. Each project is unique, and each project has further demonstrated lightning strike locations are primarily controlled by geologic factors like earth currents, and not primarily by topography, or by vegetation, or by infrastructure. In order to tie to measurement and monitoring of aquifers and subsidence, the examples selected to share in this paper are from Colorado County, Texas, and from parts of Austin, Waller, Ft. Bend, and Harris counties, Texas, as illustrated in Figure 1. Note this figure has overlaid major listric faults and salt domes (Ewing, 1990), as well as the geothermal gradient for these two areas.

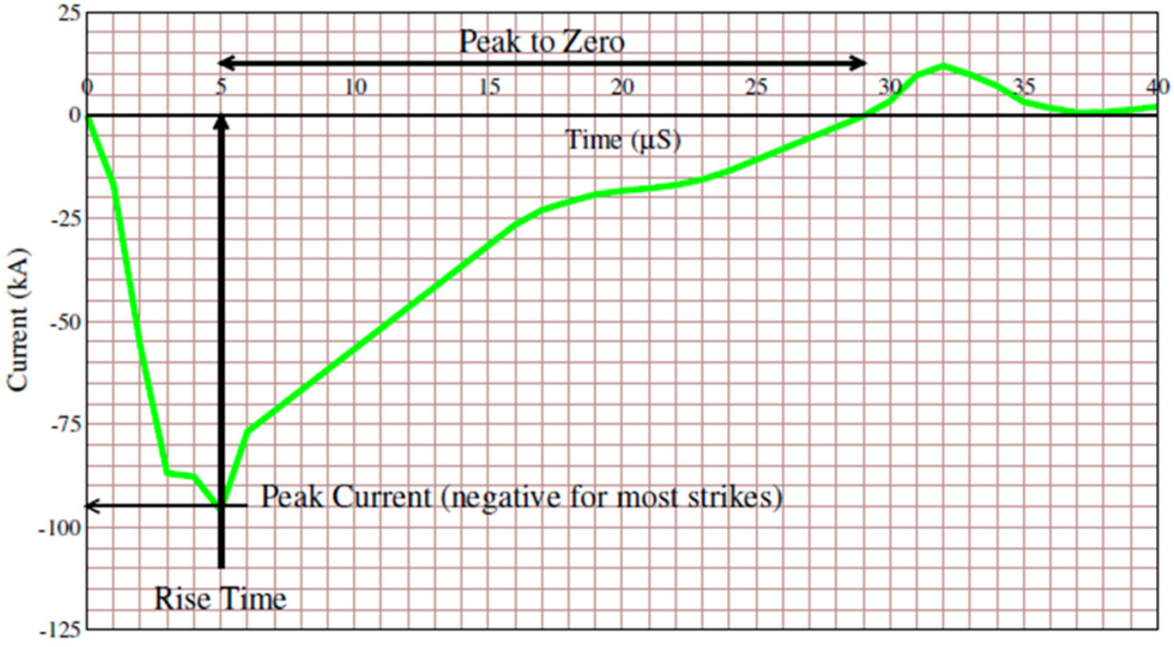

Figure 5. Cartoon of a negative lightning waveform, highlighting rise time, peak current, and peak-to-zero time.

Colorado County, Texas

Figure 7 shows a map of the rise time lightning strike attribute for Colorado County, Texas. This entire area is within the boundary of a major aquifer, namely the Gulf Coast Aquifer. The boundary of Colorado County is in brown, and the blue overlays show major listric faults from Ewing's tectonic map (1990). Note how different the rise time attribute map looks compared to the peak current map for the same area, as shown in Figure 8, and how different both of these maps look compared to the peak-to-zero time attribute map, as shown in Figure 9. Even though these maps look quite different, the density and lineament patterns within the maps are similar. Note how the overlaid faults bound areas of strong and weak lightning attribute values and trends on each different map.

On the rise time map note the consistent areas of longer rise time, more yellows and reds, along, adjacent to, and between fault boundaries. There are also longer rise time clusters along and adjacent to the northeast side of the Colorado River in this area. The shorter the rise time, the more energy there is in a typical lightning strike. The peak current map shows how the strongest measurements of peak current are on the downthrown side of the northern most listric fault on the map. The peak-to-zero time map has a similar increase in longer recorded times downthrown to this same fault. What is particularly interesting is how the peak-to-zero time cluster trends follow the faulting trends.

The differences in these maps show a difference in measurements. This could be attributed to a random nature where lightning strike occur. However, DML analysis has demonstrated from the first studies lightning strikes cluster and these clusters are somewhat consistent over time (Nelson et al., 2012). DML did find a slight correlation between positive lightning strikes and the location of oak trees in Colorado County. We do not think this correlation is related to the height of the oak trees, but rather to the electrical properties of oak trees, or their root systems, and/or the soils oak trees live in. We see this as one of many opportunities for additional research that have developed from our evaluation of using lightning data for natural resource exploration.

While there are differences in the lightning attribute maps, there are similarities in the lineaments and patterns which can be derived from the various lightning attribute maps. This is illustrated in Figures 10–12, which are the same respective lightning attributes of rise time, peak current, and peak-to-zero time as described above, only at a lead or prospect scale instead of a regional or play fairway scale. For these examples, the lightning attributes were written into a Landmark Graphics Corporation SeisWorks horizon file, and displayed as Landmark

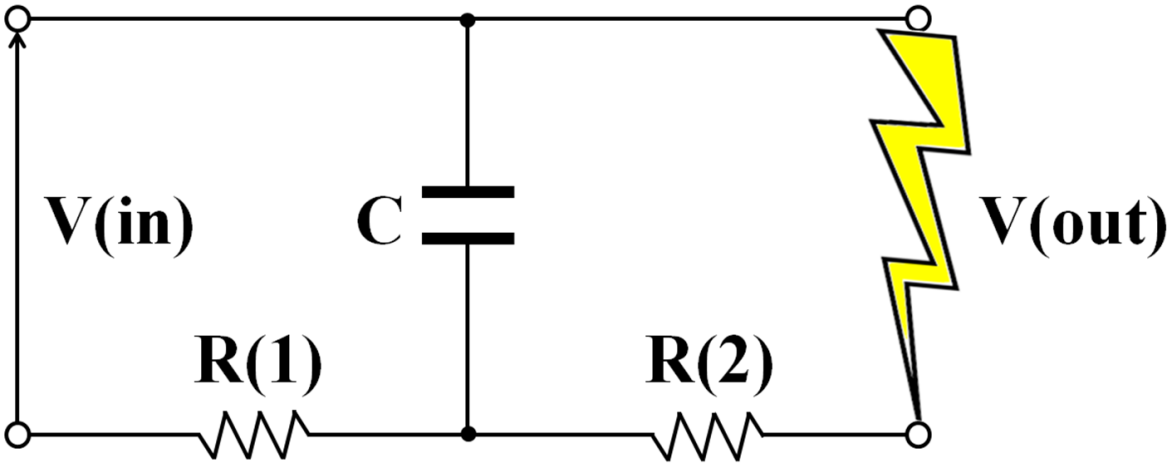

Figure 6. Lightning can be considered an RC (resistance-capacitor) circuit, where voltage (out) is the lightning stroke, and V (in) is the static charge accumulating in the thunderstorm. C is the capacitor between the bottom or top of the cloud and earth, with the atmosphere as the dielectric. R(1) is the resistance of the earth below the thundercloud as it affects the build-up of the static charge within the thundercloud. R(2) is the resistance of the earth below the cloud as it affects the movement of electrons to rebalance static charges after the lightning completes the circuit (Denham and Siebert, 2014).

Main Menu
Search
Author Index
Papers
Help

horizon files. The faults on these three figures were interpreted from a 3D seismic survey and are derivative data from this seismic interpretation. Look above the purple fault in the north across all three maps, or below the yellow fault in the middle, or on either side of the maroon fault in the south across all three maps. Also note how the seismic interpretation fault planes correlate with Ewing's faults (1990). Attribute clusters are related to the location of the faults. This consistency in the location of lightning attribute clusters provides a mechanism for breaking lightning clusters into blocks of related electrical properties, based on mapping and correlating lineaments across multiple lightning attribute maps. Our interpretation is there is a relationship between both lightning strike density and lightning attribute clusters and faults. Because lightning databases are evergreen, in that there is continual collection of new lightning data, these data can be used to measure and monitor changes and relate these changes to geologic attributes like aquifers, subsidence, and temperature gradient.

Austin, Waller, Ft. Bend, and Harris Counties, Texas

The second lightning analysis example covers over 8 salt domes in the Houston Salt Basin. The location of the analysis area is shown in Figure 1. Again, the lightning data were retrieved from the NLDN database, cleaned, normalized, and contoured. Figure 13 shows the average peak current within cells about 300 meters x 150 meters in size. One of the most noticeable anomalies on this figure is the difference in peak current on either side of the Brazos River. This difference ties with the linear Brazos Alluvial Aquifer shown in Figure 2, and with a Cretaceous transform fault, which extends to the deepwater Gulf of Mexico and was mapped by Roice Nelson as part of a proprietary regional deepwater seismic interpretation study.

Numerous lightning derived lineaments are tied to known and mapped faults in this area. This analysis extends over most of the Houston metropolitan area. There is an increase in lightning peak current, but not lightning density in downtown Houston where the tall buildings are, and the same phenomena occurs in the Galleria area where the Transco Tower is. However, there are also anomalies which are not associated with any significant infrastructure. Most importantly, the lineaments, clusters, and trends do not follow infrastructure. For instance, Figure 14 shows the lineaments and salt dome locations overlaid on a map of the part of tidal gradient when the lightning strikes occurred, and averaged over cells with an area of approximately 12,000 square meters. Figure 15 shows the lineaments and salt dome locations overlaid on a map of the density of lightning strikes during times when tidal gradient was between 75% and 100% of maximum. It is particularly interesting how these lineament patterns are relatively consistent across the different lightning attribute maps.

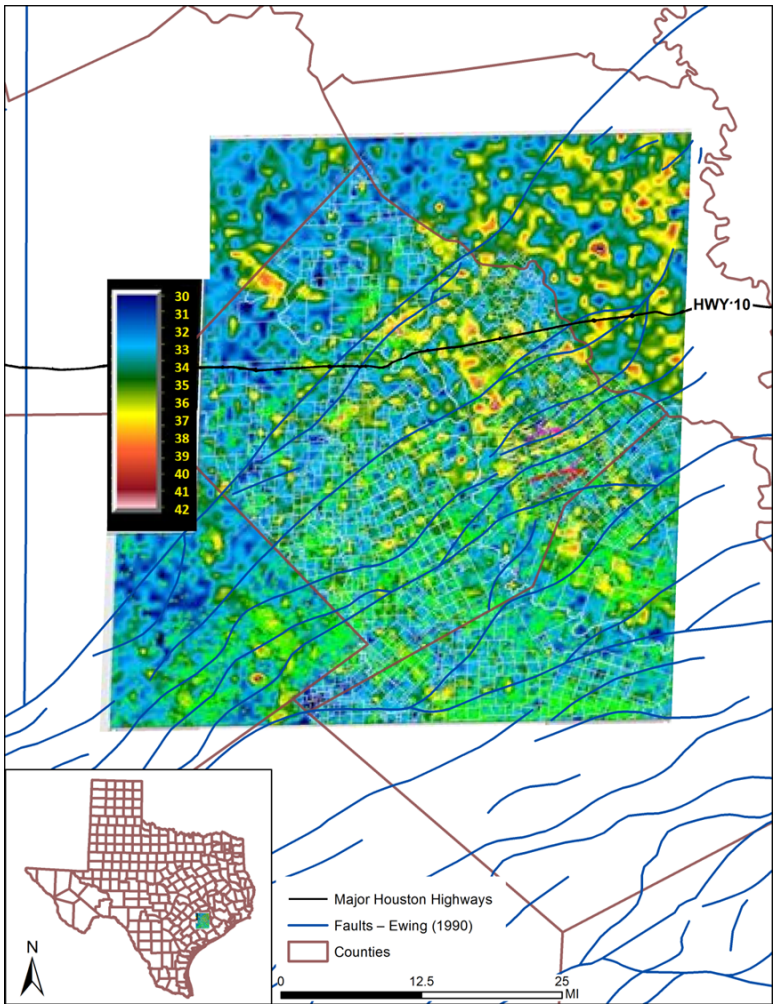

Figure 7. Rise time, Colorado County, Texas (with faults from Ewing, 1990).

In addition, we discovered there is a correlation between lightning strike attributes and temperature gradient. Figure 16 shows a cross-plot of lightning strike density and temperature gradient in degrees Kelvin for wells in this area, which wells are from 0–1500 meters depth. Note the temperature gradients from these shallow wells widely vary, and have little relationship to the lightning density. Figure 17 shows a cross-plot of lightning strike density and temperature gradient in kelvins for wells in this area which are from 1500–3000 meters depth. The temperature gradient from these intermediate depth wells has a definite correlation with lightning density. Figure 18 shows a cross-plot of lightning strike density and temperature gradient in kelvins for wells in this area which are deeper than 3000 meters depth. The temperature gradients from the deeper wells have a similar, yet slightly smaller correlation with lightning strike density. Figure 19 combines all three cross-plots onto one display, highlighting increasing correlation with the depth of the wells used to measure the temperature gradient.

Just as we did not know on the front end of this analysis whether aquifer or subsidence maps would correlate with lightning strike density, we did not know if there would be a relationship between lightning strike density and temperature gradient. High temperature gradients give low lightning density. To the extent that high temperature gradients indicate high thermal resistivity, and that this correlates with high electrical resistivity, high lightning density indicates low resistivity, and low lightning density indicates high resistivity. This correlation is most noticeable between 1500 meters and 3000 meters. This helps to explain why lightning strikes cluster, why these clusters are somewhat consistent over time, and why this can be important to natural resource exploration, specifically oil and gas within these depth ranges.

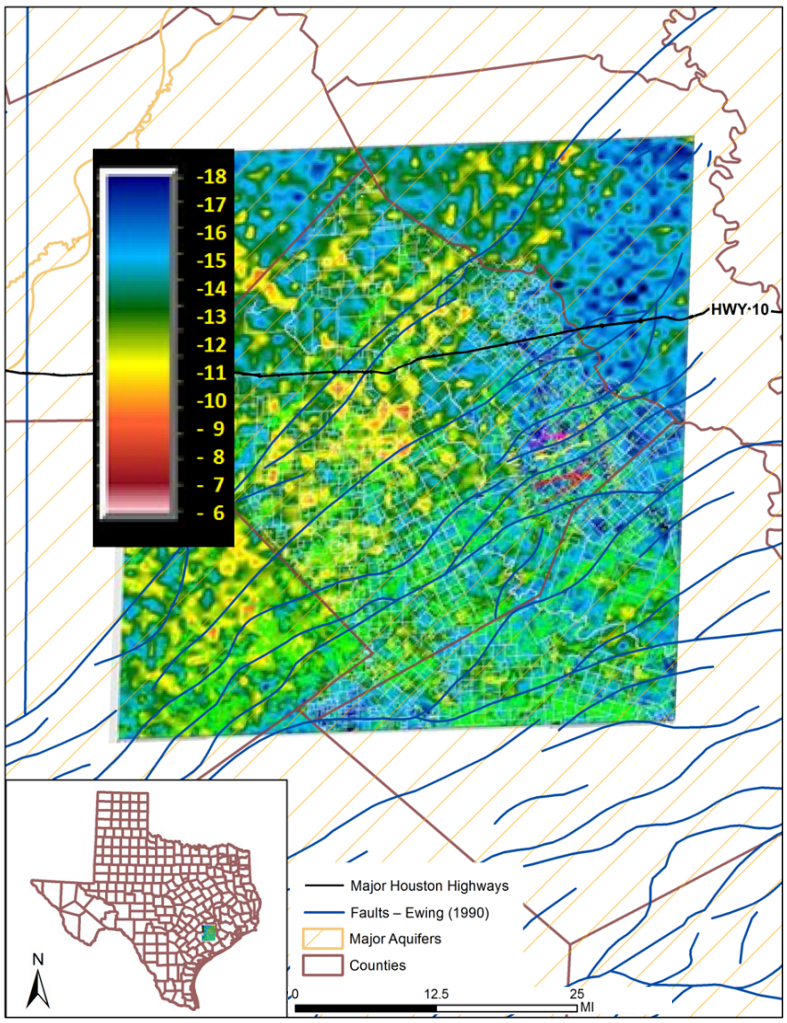

Figure 8. Peak current, Colorado County, Texas (with faults from Ewing, 1990).

SUMMARY AND CONCLUSIONS

Lightning databases provide a new geophysical data type. Like existing geophysical data types, these data can be integrated with other geophysical and geological data, including data about aquifers, subsidence, faulting, and geothermal gradient. Integration provides a better understanding of the subsurface. While there is an impact from topography, vegetation, and infrastructure on lighting strike location and attributes, the primary control on both the location and the attributes of lightning strikes are geological. These geological characteristics include resistivity, which is tied to existing methods to identify lithology, porosity, and fluid composition. While this science is new, and further advancements are expected in the coming months and decades, there is a relationship to where lightning strikes occur and geological characteristics, including within a major metropolitan area like Houston, Texas. Specifically, the correlation between temperature gradient between 1500 meters and 3000 meters and lightning strike density demonstrates lightning strike locations are not tied to the very shallow depths of penetration (skin depth), but rather to geologic and electrical properties which are at oil and gas exploration depths. The analysis is just beginning.

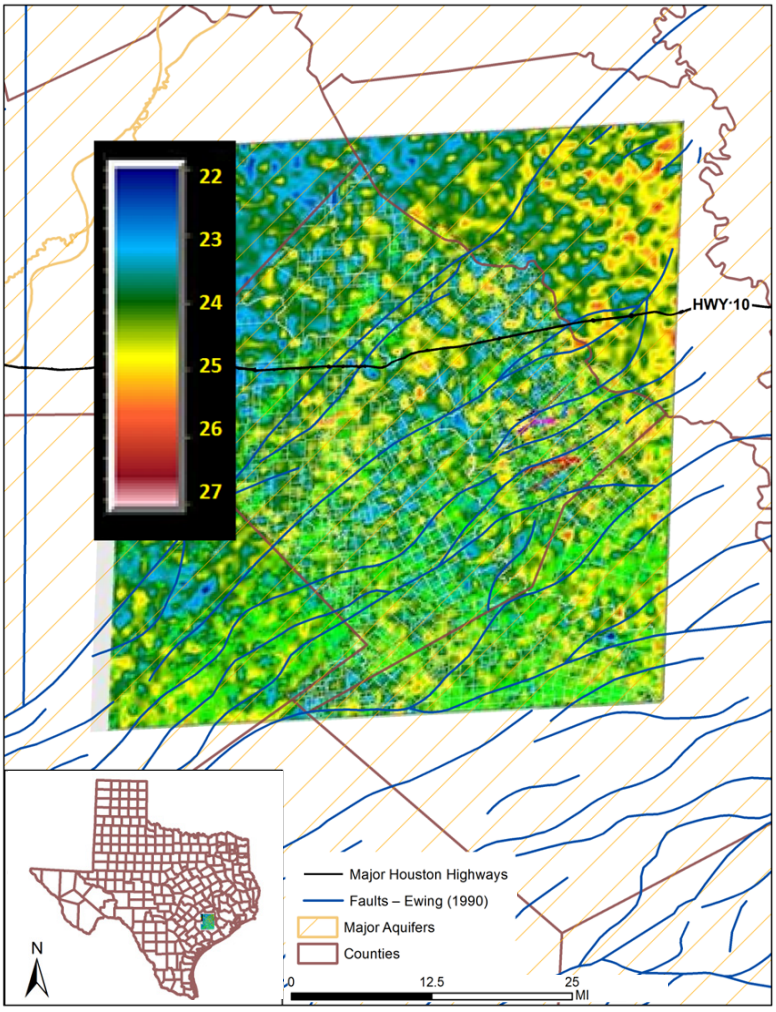

Figure 9. Peak-to-zero time, Colorado County, Texas (with faults from Ewing, 1990).

ACKNOWLEDGMENTS

Susan C. Horvath and Shadiya M. Bello of Global GIS Analytic Consulting, LLC. based in Austin, Texas for finding and providing temperature data and the basement fault overlays from the Bureau of Economic Geology in Austin, Texas, and for helping put figures together for this paper together to meet GCAGS guidelines.

REFERENCES CITED

Baba, Y., and V.A. Rakov, Influence of strike object grounding on close lightning electric fields: Journal of Geophysical Research, p. 113, D12109, doi:10.1029/2008JD009811.

Cagniard, L., 1953, Basic theory of the magneto-telluric method of geophysical prospecting: Geophysics, 18, p. 605–635.

Denham L. R., H. R. Nelson, Jr., and D. J. Siebert, 2013, Lightning data and resource exploration: Society of Economic Geologists Convention, Houston, Texas.

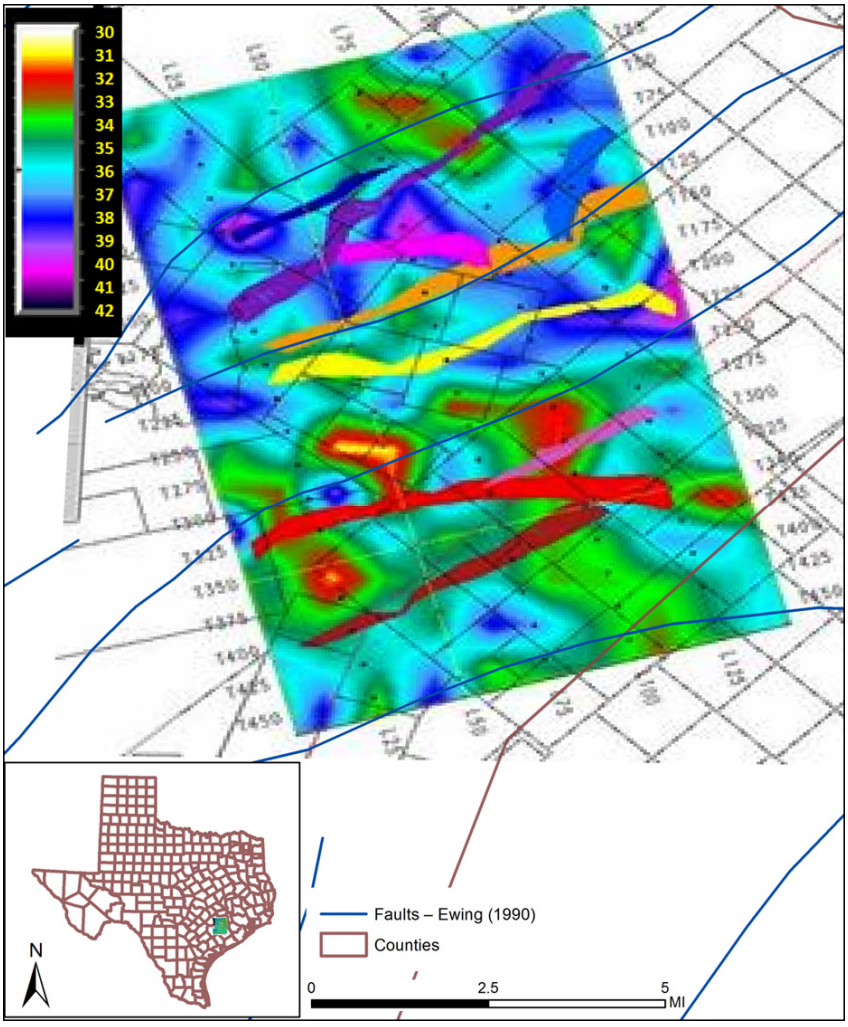

Figure 10. Rise time, 3D seismic survey area, Colorado County, Texas (with faults from Ewing, 1990).

Denham, L. R., and D. J. Siebert, 2014, Separating geology and meteorology: Abstract submitted to the Society of Economic Geologists, for presentation at the convention in Denver, Colorado.

Ewing, T. E., 1990, Tectonic map of Texas (4 sheets, scale 1:750,000) / Tectonic framework of Texas (36 p.): Texas Bureau of Economic Geology, Austin.

George, P. G., R. E. Mace, and R. Petrossian, 2011, Aquifers of Texas: Texas Water Development Board Report 380, Austin, 172 p.

Haggar, K. S., 2014, Coastal land loss and landscape level plant community succession: An expected result of natural tectonic subsidence, fault movement, and sea level rise: Gulf Coast Association of Geological Societies Transactions, v. 64, p. 139–159.

Hembury, N., and R. Holle, 2011, Flash of inspiration—Latest innovations in worldwide lightning detection: Meteorological Technology International, April 2011 issue, p. 48–50, <http://www.vaisala.com/Vaisala%20Documents/White%20Papers/Flash_of_Inspiration_MTI_article_April2011.pdf> Last accessed September 17, 2014.

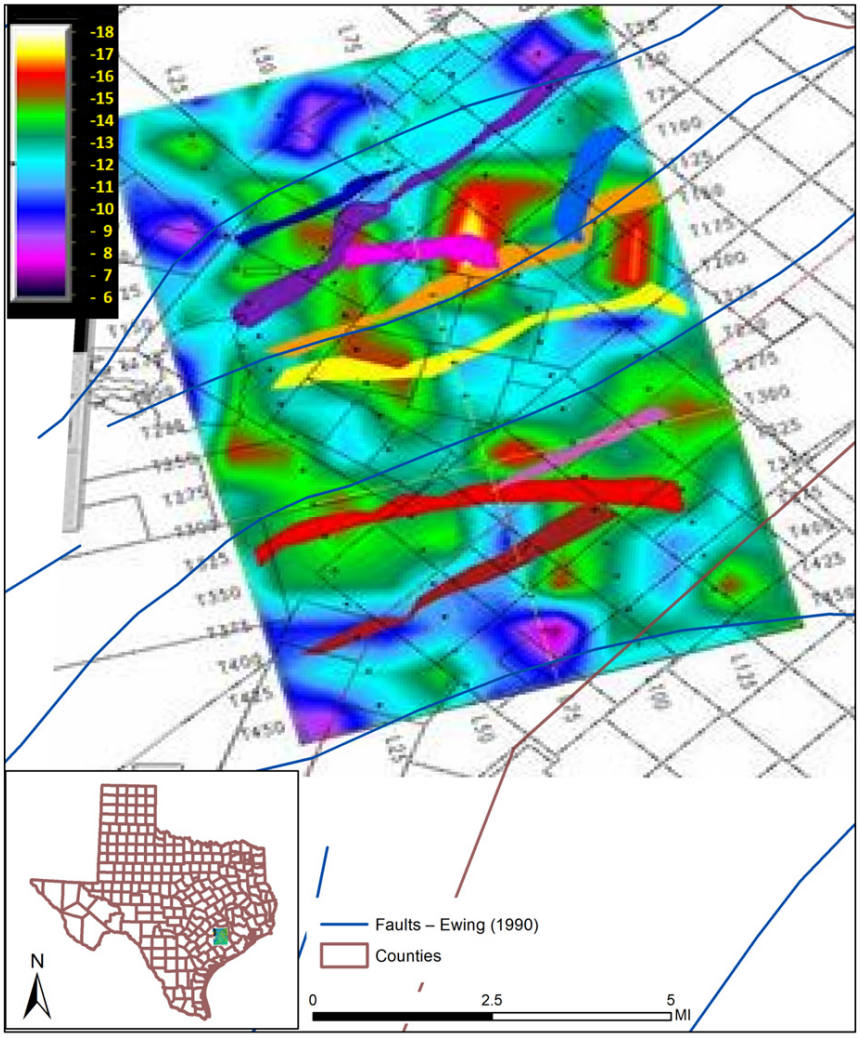

Figure 11. Peak current, 3D seismic survey area, Colorado County, Texas (with faults from Ewing, 1990).

Houston Galveston Subsidence District, 2000, Subsidence, 1906–2000, <http://mapper.subsidence.org/Static%20Maps/SubsidenceMap1906-2000.pdf> Last accessed September 17, 2014.

Jin, X. B., Z. M. Chen, Q. M. Ma, Y. L. Li, and J. W. Pu, 2013, The correlations between the lightning density distribution of Sichuan Province and the seismic area: International Journal of Geosciences, v. 4, p. 380–386, doi:10.4236/ijg.2013.42036.

Murphy, M. J., R. L. Holle, and N. W. S. Demetriades, 2008, Cloud-to-ground lightning warnings using electric field mill and lightning observations: Proceedings of the 20th International Lightning Detection Conference, Tucson, Arizona.

Nelson, H. R., Jr., D. J. Siebert, and L. R. Denham, 2012, Lightning data—The new EM "seismic" data: Presented at the EM Workshop, Society of Economic Geologists Convention.

Nelson, H. R., Jr., D. J. Siebert, and L. R. Denham, 2013, Lightning data, a new geophysical data type: American Association of Petroleum Geologists Annual Meeting, Pittsburg, Pennsylvania.

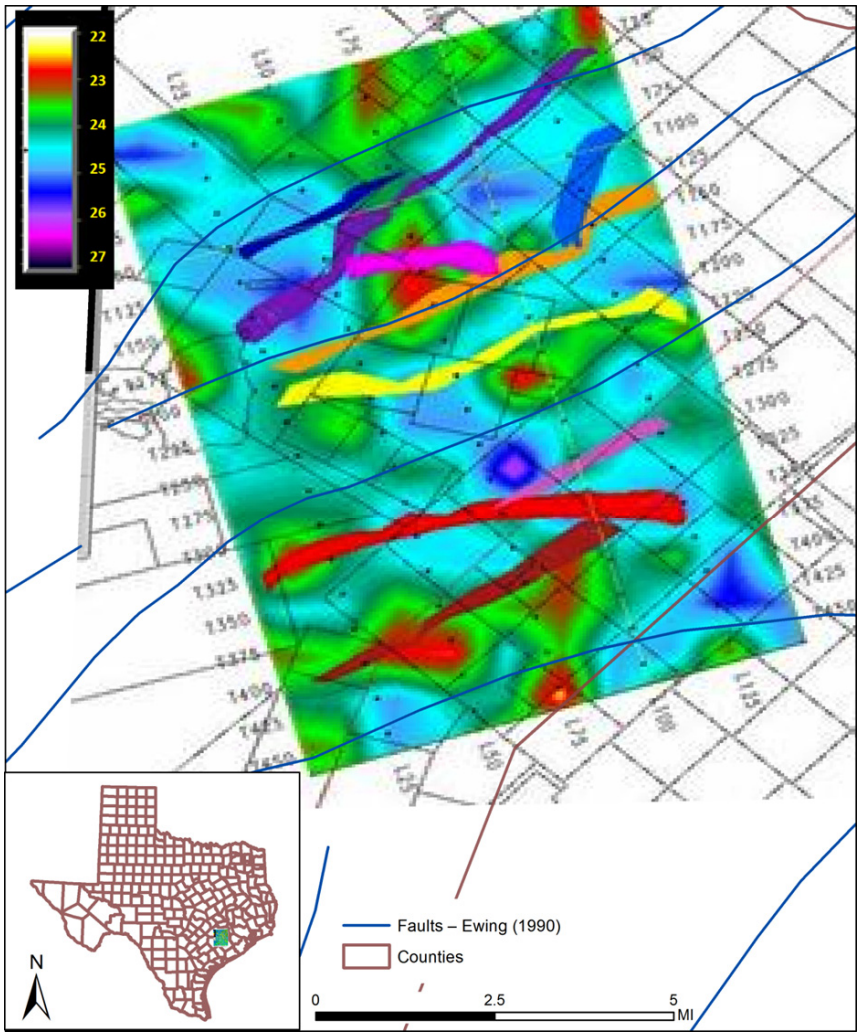

Figure 12. Peak-to-zero time, 3D seismic survey area, Colorado County, Texas (with faults from Ewing, 1990).

Nelson, H. R., Jr., D. J. Siebert , and L. R. Denham, 2014, Telluric and earth currents, lightning strike locations, and natural resource exploration: American Association of Petroleum Geologists Annual Meeting, Houston, Texas.

Orville, R. E., 2008, Sparked by technology—The history of the national lightning detection network: American Meteorological Society Bulletin, v. 89.2, p. 180–190.

Rakov, V. A., and M. A. Uman, 2003, Lightning: Physics and effects: Cambridge University Press, U.K., 687 p.

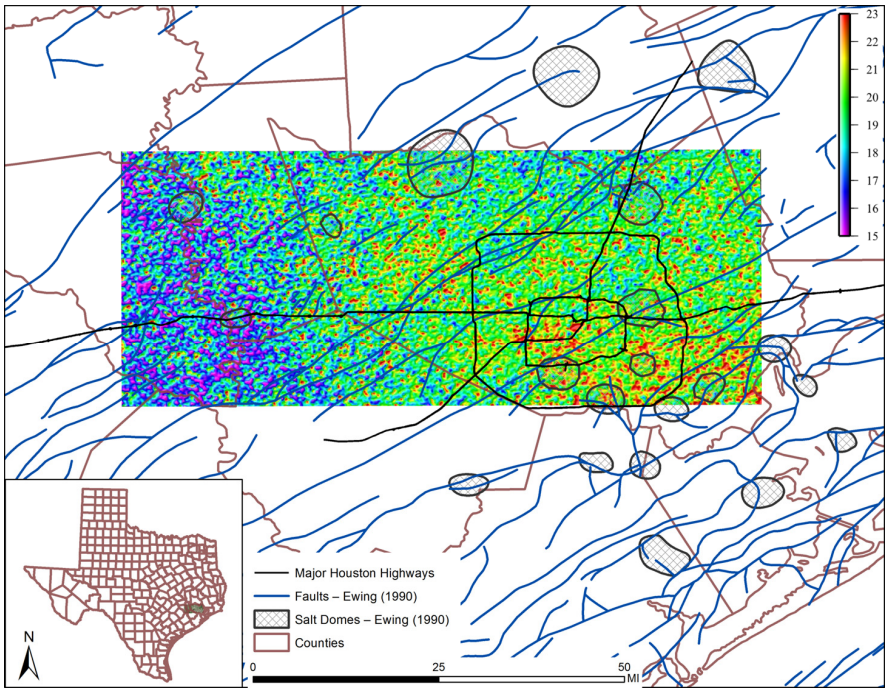

Figure 13. Average peak current over parts of Austin, Waller, Ft. Bend, and Harris counties, Texas, from 2000–2011 (with faults and salt domes from Ewing, 1990).

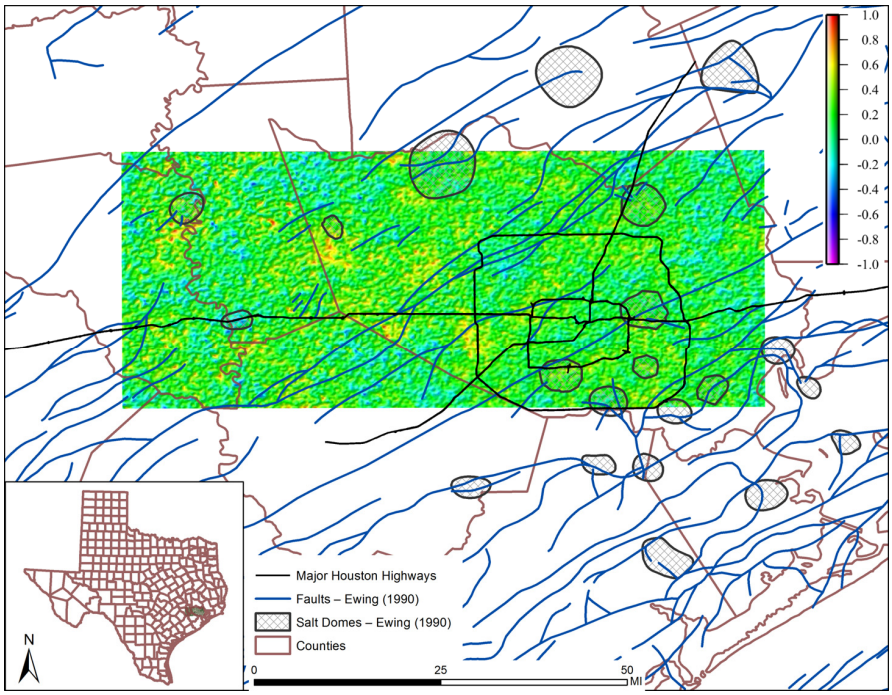

Figure 14. Tidal gradient when lightning strikes occurred in parts of Austin, Waller, Ft. Bend, and Harris counties, Texas, from 2000–2011 (with faults and salt domes from Ewing, 1990).

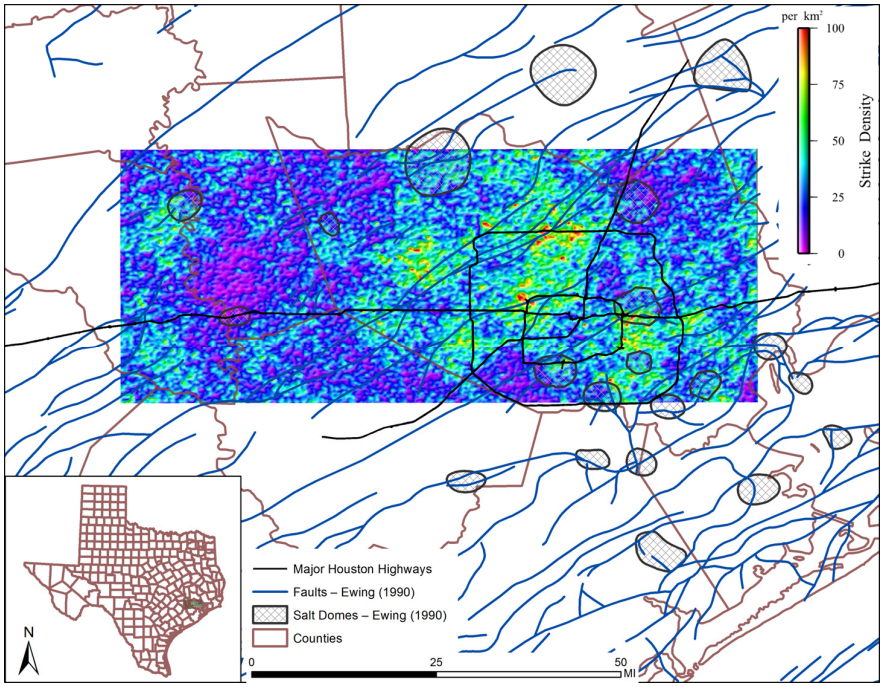

Figure 15. Lightning strike density (strikes per square kilometer) at high tide gradient in parts of Austin, Waller, Ft. Bend, and Harris counties, Texas, from 2000–2011 (with faults and salt domes from Ewing, 1990).

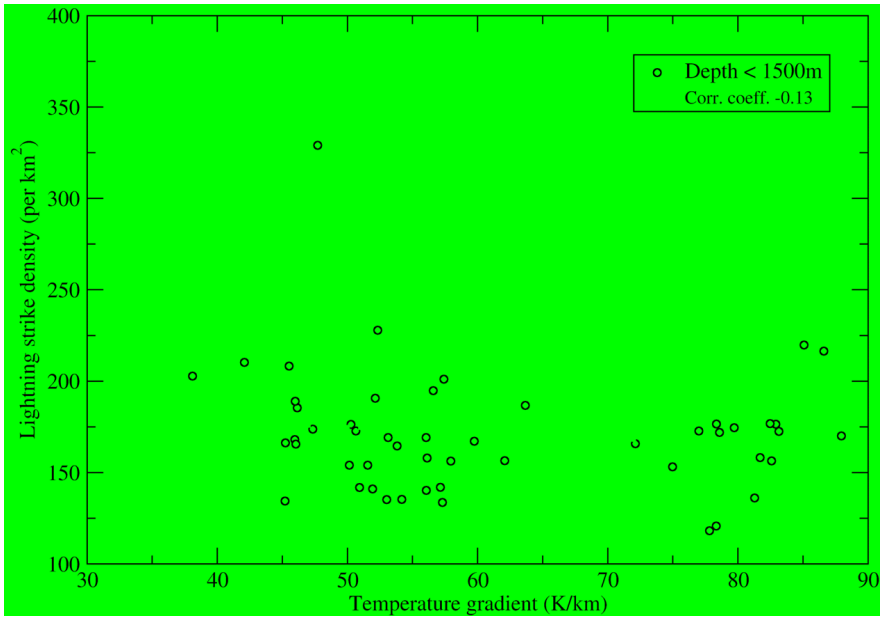

Figure 16. Lightning strike density (strikes per square kilometer) at wells vs. temperature gradient in kelvins per kilometer, from wells drilled between 0–1500 meters in depth in parts of Austin, Waller, Ft. Bend, and Harris counties, Texas. Lightning strike density is computed from the number of strikes (2000–2011) in cells 10” longitude by 5” latitude, with an aerial Gaussian filter of 1.0 kilometer width at 6σ applied to the resulting grid.

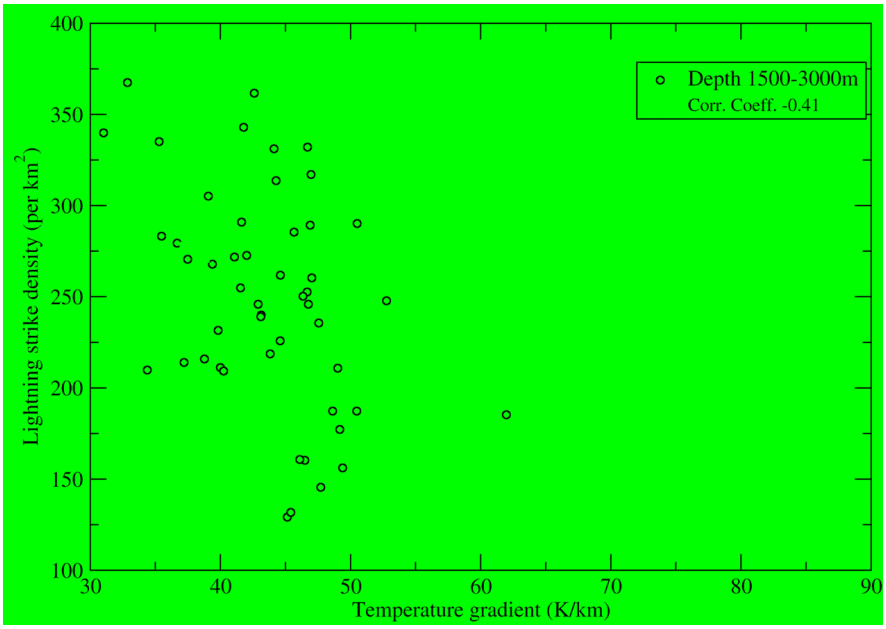

Figure 17. Lightning strike density (strikes per square kilometer) at wells vs. temperature gradient in kelvins per kilometer, from wells drilled between 1500–3000 meters in depth in parts of Austin, Waller, Ft. Bend, and Harris counties, Texas. Lightning strike density is computed from the number of strikes (2000-2011) in cells 10” longitude by 5” latitude, with an aerial Gaussian filter of 1.0 kilometer width at 6σ applied to the resulting grid.

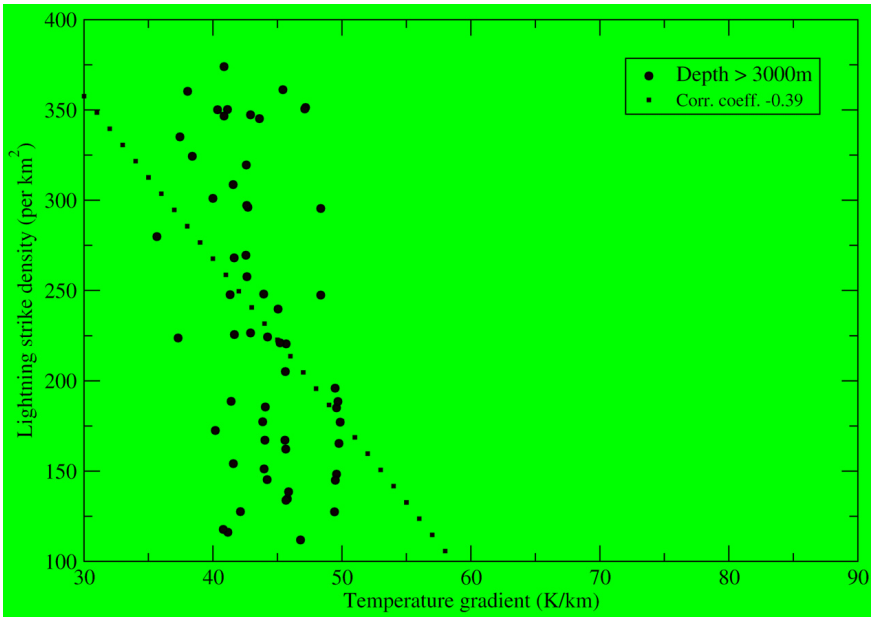

Figure 18. Lightning strike density (strikes per square kilometer) at wells vs. temperature gradient in kelvins per kilometer, from wells drilled greater than 3000 meters in depth in parts of Austin, Waller, Ft. Bend, and Harris counties, Texas. Lightning strike density is computed from the number of strikes (2000-2011) in cells 10” longitude by 5” latitude, with an aerial Gaussian filter of 1.0 kilometer width at 6σ applied to the resulting grid.

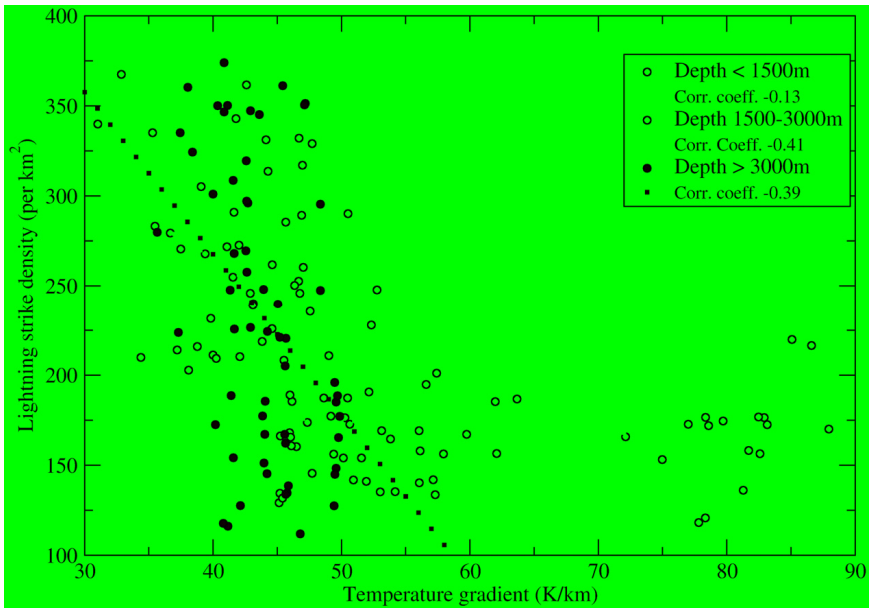

Figure 19. Lightning strike density (strikes per square kilometer) at wells vs. temperature gradient in kelvins per kilometer, from wells drilled in parts of Austin, Waller, Ft. Bend, and Harris counties, Texas. Lightning strike density is computed from the number of strikes (2000–2011) in cells 10” longitude by 5” latitude, with an aerial Gaussian filter of width of 1.0 kilometer width at 6σ applied to the resulting grid.

NOTES